ELSEVIER

Contents lists available at ScienceDirect

Clinical Biomechanics

journal homepage: www.elsevier.com/locate/clinbiomech



Biomechanics study of a 3D printed sacroiliac joint fixed modular hemipelvic endoprosthesis



Xinyu Li^{a,c}, Tao Ji^{b,*}, Siyi Huang^b, Caimei Wang^c, Yufeng Zheng^a, Wei Guo^{b,*}

- ^a College of Engineering, Peking University, Beijing 100871, China
- b Musculoskeletal Tumor Center, People's Hospital, Peking University, Xizhimen Nan 11#, Xicheng District, Beijing 100044, China
- ^c Beijing 3D Printing Orthopedic Application Engineering Technology Research Center, Beijing 102200, China

ARTICLE INFO

Keywords: Strain distribution Pelvic prosthesis Biomechanics Periacetabular tumor

ABSTRACT

Background: Reconstructing pelvic type II + III defect caused by bone tumors is challenging. The purpose of this study was to explore the *in vitro* biomechanical properties of a reconstructed pelvis after periacetabular resection using three-dimensional (3D) printed sacroiliac joint (SIJ) fixed modular hemipelvic endoprosthesis.

Methods: Type II/II + III pelvic resection was simulated on an artificial pelvic model. The bilateral acetabulum and pubis were constrained, and the pelvis was maintained in a human physiological standing position. A vertically continuous linear load was applied on the upper face of S1 until obvious unloading or fixed failure occurred. A noncontact optical 3D strain measuring system was used to measure the strains and displacements at the selected area.

Findings: The strain at the points of interest did not obviously differ between the intact and reconstructed pelvis models. The difference in the displacement on the reconstructed side was 0.237 mm, and that on the contralateral side was 0.245 mm. The maximum differences in the displacement at the acetabulum were 0.209 mm (vertical) and 0.324 mm (horizontal). A crack at the superior rim of the contralateral acetabulum occurred, and failure loading of 7.126 kN.

Interpretation: The prosthesis in this study showed satisfactory mechanical properties and structural stability. According to the mechanical evaluations, the 3D printed sacroiliac-stabilized hemipelvic endoprosthesis can be used to reconstruct a stable acetabular structure, and there was little influence on the mechanical properties of the surrounding bone structures. The prosthesis design is reasonable, and the mechanical distribution on the reconstructed side was similar to that on the contralateral side.

1. Introduction

The pelvis is one of the most important support structures in the human body. The pelvis helps stabilize and protect the organs. Unlike long bones (the femur and tibia), which have thick cortical bone and canal structure because they endure large axial loads, the pelvis consists mainly of low-density cancellous bone, and the pelvis is only covered by a thin layer of cortical bone. A previous study found that the force experienced by the pelvis of an individual during walking was 3 times larger than his or her body weight (Bergmann et al., 2001).

Pelvic tumors constitute a severe orthopedic disease, and it is particularly challenging for orthopedists to perform resection and reconstruction after removing pelvic tumors. Some metastatic deposits are associated with an instability of the acetabulum due to bony invaded by tumor tissue, which may cause severe pain and functional

disability. The focus of treatments should be to relieve pain and restore function for as long as possible (Harrington, 1981). Many reconstruction methods are available for pelvic structures (Aboulafia et al., 1995). The saddle, custom-made prostheses, modular prostheses, and the Schoellner pedestal cup are used most often (Aljassir et al., 2005; Enneking and Dunham, 1978; Falkinstein et al., 2008; Guo et al., 2007; Natarajan et al., 2001). Pelvic prostheses still lack well-established design principals. Some pelvic prostheses are unstable and prone to loosening after implanted for a couple of years (Cottias et al., 2001; Hillmann et al., 2003; Uchida et al., 1996; Windhager et al., 1996). A 3D-printed hemipelvic endoprosthesis has been reported to be used after type II/II + III resections. Its design evolved from that of a previous hemipelvic prosthesis (Ji et al., 2013). A 3D-printed modular hemipelvic endoprosthesis of a size was selected intraoperatively to fit the defect after the tumor was removed. Before definitive fixation, the

E-mail addresses: jitaomd@163.com (T. Ji), bonetumor@163.com (W. Guo).

^{*} Corresponding authors.

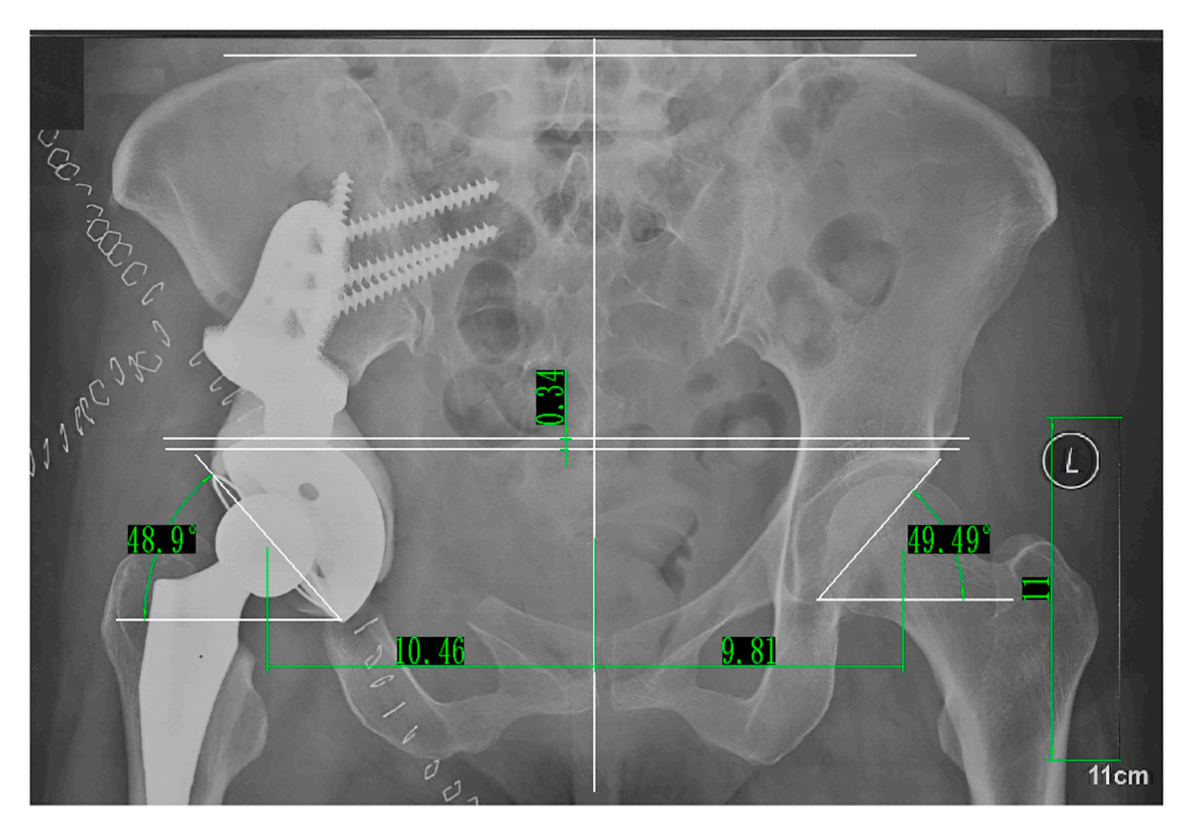


Fig. 1. a Postoperative radiograph.

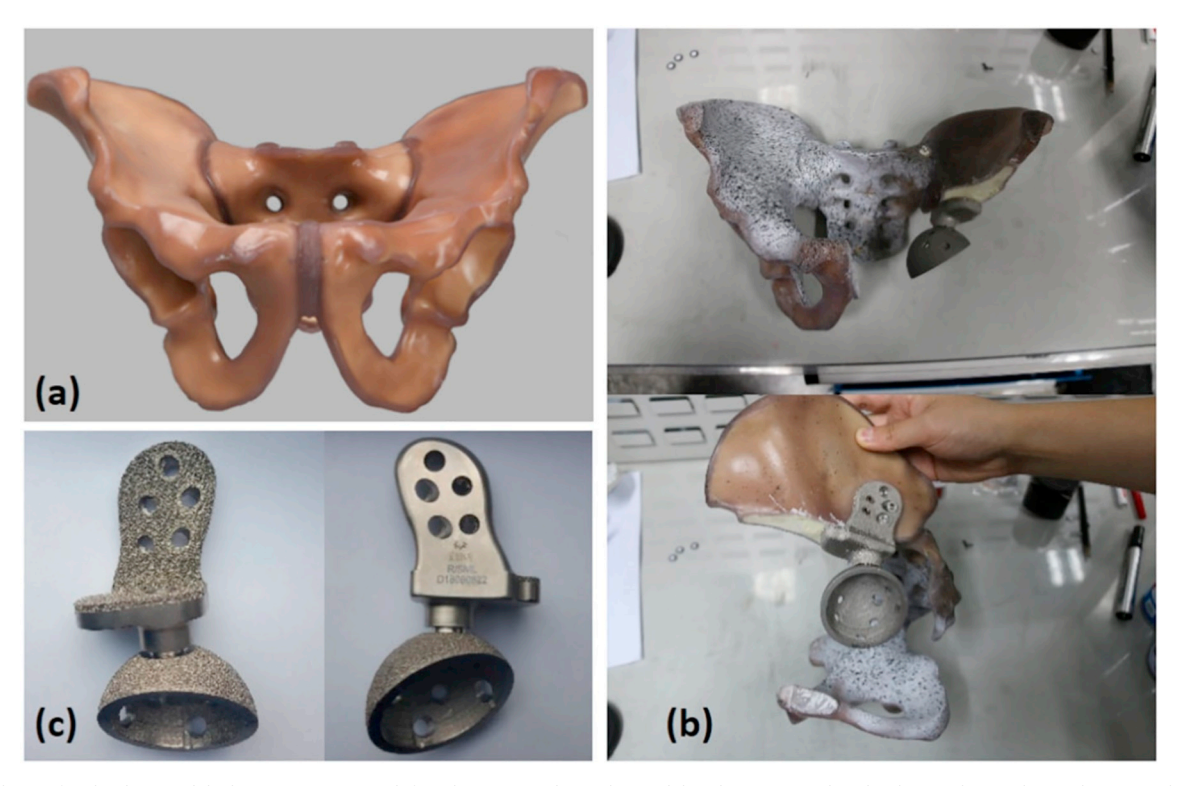


Fig. 2. (a) The artificial pelvis model; (b) an II + III area defect that was made on the model and restructured with a hemipelvic endoprosthesis; (c) the mentioned hemipelvic endoprosthesis.

antervesion and inclination of the acetabular cup was adjusted, and three cancellous screws were introduced through the screw holes across the sacroiliac joint into the vertebral body of S1 or S2. Another two more cortical screws were used to strengthen the fixation. High viscosity bone cement containing gentamicin was used to augment the prosthesis, and the hip joint was restored, as in a total hip arthroplasty. It has been shown that the prosthesis can yield good limb salvage outcomes in clinical practice, as shown in Fig. 1.

Although 3D-printed modular hemipelvic endoprostheses can mimic the pelvis in its physiological structure, we still need to evaluate the mechanical performance of the prosthesis. Few research studies on the mechanical performance of prostheses have been conducted with the use of *in vitro* experiments. It is difficult to comprehensively evaluate the effectiveness of a pelvic prosthesis using traditional methods due to the complex geometry of the pelvic bones. The mechanical properties of cadaveric pelvises are heterogeneous. Therefore, it is less rigorous to assess the effectiveness of a pelvic prosthesis under a uniform, standard test. Recently, with the advancements in artificial pelvic models and digital image measurement technology, the test method has been improved sufficiently to allow researchers to evaluate the performance of pelvic prostheses in a mechanical laboratory (Xu et al., 2018).

The aim of this study was to evaluate the mechanical performance of a 3D-printed modular hemipelvic endoprosthesis that was implanted in a standard, artificial pelvic model. The entire pelvic ring, including the reconstructed part and contralateral side, was considered the focus area in this study. The strains and displacements at particular points on the pelvic ring were used as the indices to evaluate the mechanical properties and stability of the pelvic prosthesis.

2. Methods

2.1. Specimens

An artificial composite pelvic model with standard mechanical properties was used in this research (#3415 Sawbones USA). A porous material, similar to cancellous bone, was used inside the pelvic model, and a dense material, similar to cortical bone, was used on the surface of the model (Fig. 2a). Anisotropic materials were used in the pelvic model to simulate the normal physiological pelvis. To simulate type II/ II + III resections, an osteotomy and implant fixation was performed by the senior author (JT); the reconstructed pelvis is shown in Fig. 2b. A three-dimensional (3D)-printed standard hemipelvic endoprosthesis (AK Medical Co., Beijing, China) was used to reconstruct the pelvic ring (Fig. 2c). This hemipelvic prosthesis was manufactured by a 3Dprinting technology that is widely known as EBM. The prosthesis contained three components: an acetabular cup, ilium fixation part, and screws. The iliac fixation part had an anatomical matched shape that was identical to the lateral cotrex of ilium, which can better fit the surface of the iliac bone after the osteotomy and provide initial stability. In addition, a 3D-printed porous structure was used as the osseointegration surface at the bone-implant interface which providing bone ingrowth microstructure and initial postoperative stability was provided by the screws (Xiu et al., 2016).

2.2. Application of load

The pelvic model was mounted on a steel structure to simulate the individual in a standing position. The pelvic model was set on the fixture with the prosthetic femoral stem fixed in all directions. The anterior part of the pubis was also hooked by a fixed hook to prevent sagittal rotation of the pelvic model. It was ensured that the pelvis was in a standing position by adjusting the length of the hook. A load was applied through a bone cement block on the upper face of S1 by a mechanical testing machine (Instron USA). The vertical load was increased linear incrementally from 0 N to 600 N (with 50-N intervals). The load was first applied on the intact pelvis, and the mechanical performance was compared with that of the cadaveric pelvis, which was placed under the same load in a previous study (Hao and Zhixiu, 2011) to verify the effectiveness of using an artificial pelvic model (Fig. 3). After the test with the artificial pelvic model was performed, a unilateral osteotomy and reconstruction with the hemipelvic endoprosthesis were performed, and the same load condition was applied on the reconstructed pelvis. To test the maximum bearing capacity of the pelvic ring structure after the implantation of the prosthesis, a gradually

increasing vertical load was applied until structural failure.

The strains around the contralateral acetabulum on the intact and reconstructed pelvic model were measured to study the effects of implanting the prosthesis on the contralateral side. To assess the influence of the implant on the reconstructed area, the strain in the iliac osteotomy plane on the reconstructed side and that in the same area on the contralateral side were compared. By comparing the displacements of the left and right acetabulum under the vertical direction, the stability of the hemipelvic endoprosthesis was evaluated. The stability of the pelvis after reconstruction was assessed *via* the displacements of the bilateral acetabulum.

2.3. Measurement method

The strain and displacement of the pelvic model were recorded by a noncontact optical 3D strain measuring system using digital image correlation (DIC) technology with an ARAMIS 6 M 75 mm (GOM, Germany). Image recognition was performed by two digital cameras to analyze and compare the digital images and form a 3D image (Fig. 4a). By tracing a randomly applied high-contrast speckle pattern using blue light, the strain and displacement within the specimen were calculated from these images (Fig. 4b). The initial imaging process was used to define unique areas identified by a large number of pixels (15 to 30), which are known as macroimage facets. Each facet was considered a measurement point (Xu et al., 2018). These measured facets were tracked in each successive image, and the strain on the pelvis was calculated by comparing the digital images at different vertical loads. To maximize the number of successive facets and minimize the number of missing measurements in this test, the frequency of exposure was set at 3 Hz, and the resolution of these images was 2448 imes 2050 pixels. The test images were processed by GOM Correlate software (GOM Correlate 2017, Germany).

2.4. Statistical analysis

Statistical analyses were performed with SPSS software (version 16.0, Chicago, IL, USA). The data of the intact and reconstructed pelvis were compared. The difference between the two groups of data was calculated and analyzed as a new group of data, and the average value and standard deviation (SD) of the new data were analyzed to reflect the difference before and after reconstruction. The smaller the average value and standard deviation, the closer the mechanical response was between the intact and reconstructed pelvis.

3. Results

3.1. Model validation

According to the physiological structure of the intact pelvis, the load was transmitted down to the acetabulum along the pelvic ring and ischial notch. The strain along the entire pelvic ring and ischial notch is shown in Fig. 5a and Fig. 5b. The arrow shows the direction of the main strain. It was obvious that the direction of strain was the same as the load transfer path of the pelvis. In Fig. 5b, the strain traveled along the pelvic ring, indicating that the mechanical characteristics of the artificial pelvis mimic those of a human pelvis. The pelvic bone was a sandwich structure, which means that the load in the pelvic bone was transferred through the cortical shell (Dalstra and Huiskes, 1995). Some previous studies have established accurate pelvic models (Anderson et al., 2005). In these studies, the stress levels at the acetabulum, iliopectineal line, and sciatic notch of the pelvis were higher when the individual was static than when he or she was walking.

The strain values at particular points on this artificial pelvis model were compared with those on the cadaveric pelvis under the same loading condition (550 N). Six points on the surface of the pelvis were chosen as the measuring points on the basis of previous research: (1) the

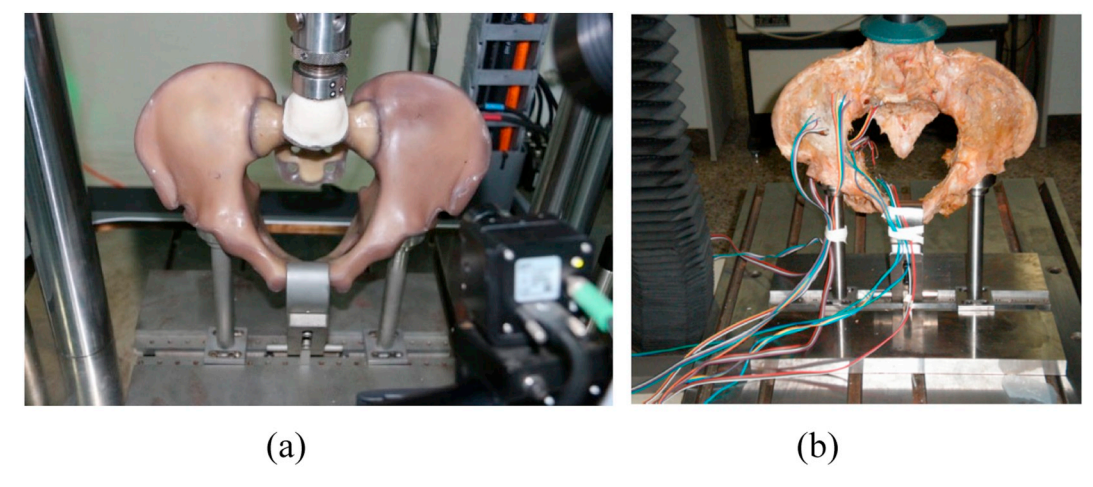


Fig. 3. (a) The artificial pelvis was fixed to the machine in a standing position using a special component; (b) the *in vitro* experiment of the pelvis was performed to obtain strain values at the measurement points (Hao and Zhixiu, 2011).

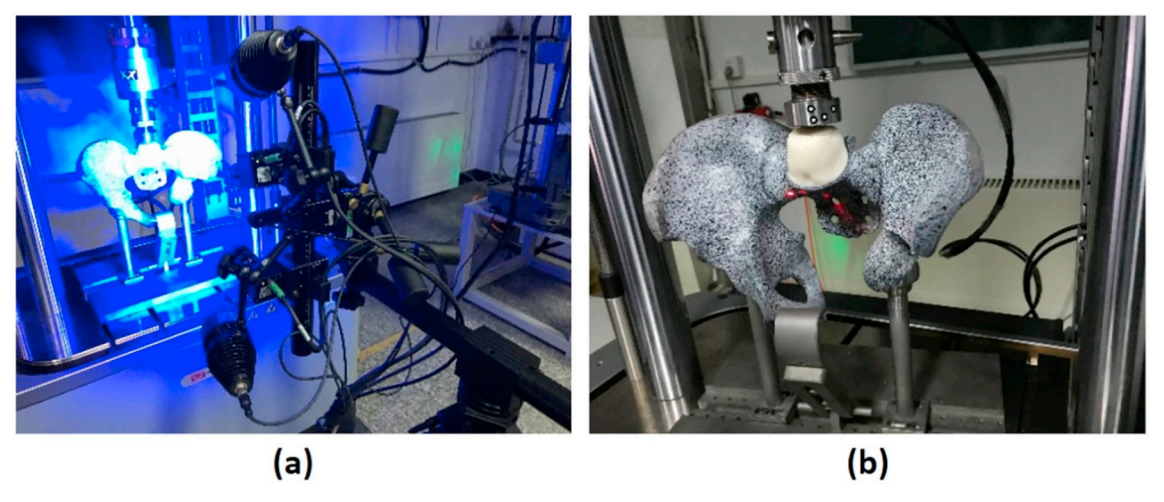


Fig. 4. (a) The 3D structured light emitted by the DIC system is evenly scattered on the surface of the measured object; (b) a randomly distributed high-contrast speckle pattern was sprayed on the pelvic model.

midpoint of the iliopectineal line; (2) the central point of the acetabular inner plate; (3) the point on the sacral 1st vertebrae near the sacroiliac joint; (4) the point on the ilium of the sacroiliac joint as high as the sacral 1st vertebrae; (5) the iliac fossa; and (6) the highest point of the ischial notch (Hao and Zhixiu, 2011). The results are shown in Table 1. Although the artificial pelvis model has a similar mechanical distribution to the physiological pelvis, there are still differences in the material properties between the artificial material and natural bone tissue (Girardi et al., 2016). According to the strains shown in Table 1, the strain value at each point varies greatly. To better demonstrate the trend in the variation of the strain among the points and to compare the mechanical properties between the artificial pelvic model and physiological pelvis, the strain values were normalized by the researchers. The minimum strain was taken as the benchmark, and strains were normalized, as shown in Fig. 6. The normalized strains at some points were smaller than those in the cadaveric pelvis (Hao and Zhixiu, 2011), indicating that the artificial pelvic model has a lower stiffness than cadaveric pelvis at points 3, 4 and 6. This result suggests that the cadaveric pelvis has a stronger sacroiliac joint and ischial notch structure than the artificial pelvic model. However, the overall trends of the normalized strain were similar between the artificial pelvic model and the cadaveric pelvis. According to the normalized strain values, the mechanical conduction path is the sacroiliac joint, the iliopectineal line, and the ischial notch, the acetabulum. The mechanical performance of the artificial pelvic model was the same as that of the physiological pelvis.

3.2. Strain distribution

In the DIC measurement results, the mean strain in the supra-acetabular area was selected as the strain at 3 mm above the acetabulum. The strain at 3 mm above the acetabulum on the contralateral side was compared between the intact and reconstructed pelvis under the same loading condition (Fig. 7). Obviously, with an increase in the load, the trend and magnitude of the strain above the acetabulum were similar before and after reconstruction. The strains at 3 mm above the acetabulum on the intact and reconstructed pelvic models were 2.17e-4 (0.509) and 2.03e-4 (0.340), respectively, at 600 N. The average value (SD) of the difference between the two groups of data was 1.408e-4 (1.329e-3), which was narrow illustrating that the difference in the strain on the contralateral side before and after reconstruction was not significant.

Similarly, we also compared the strain at 3 mm above the bone osteotomy plane between the reconstructed side and contralateral side (Fig. 8). Regarding the differences between the two sets of data, the average value (SD) of the difference between the two groups of data was 1.344e-3 (1.772e-3). The strain of the bone structure near the reconstructed region was similar to that of the contralateral side. This result indicated that the prosthesis recovered the pelvis with rational loading restoration.

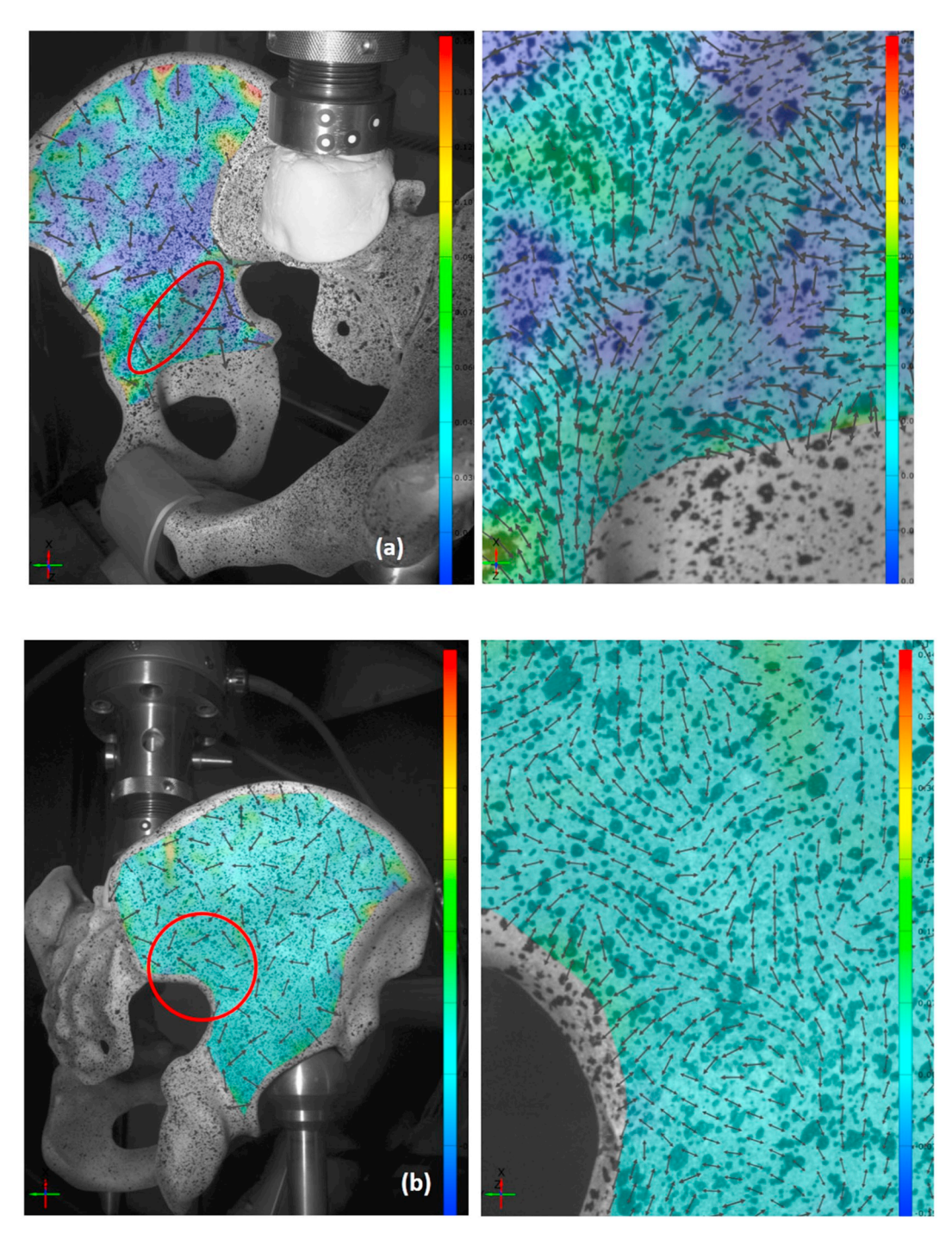


Fig. 5. The principal direction of strain when the pelvic model is under pressure. The arrow shows the direction of the main strain. a, the arcuate line; b, the greater sciatic notch.

Table 1
The strains at six points on the pelvis.

Measuring points		Cadaveric pelvis (Hao and Zhixiu, 2011)	Artificial pelvis
1	The midpoint of the iliopectineal line	5.60e – 04	1.10e – 04
2	The central point of the acetabular inner plate	3.35e-04	0.80e - 04
3	The point on the sacral 1st vertebrae near the sacroiliac joint	1.81e-03	1.18e - 03
4	The point on the ilium of the sacroiliac joint as high as the sacral 1st vertebrae	5.62e-04	4.50e - 04
5	The iliac fossa	4.17e-04	0.70e - 04
6	The highest point of the ischial notch	2.50e - 04	3.50e - 04

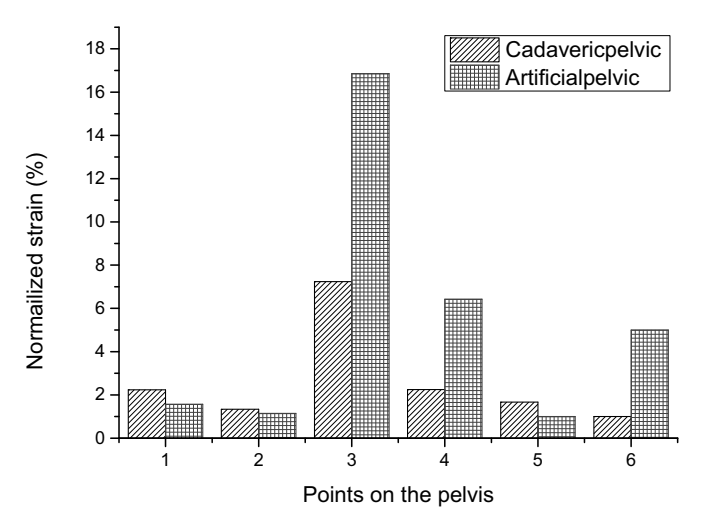


Fig. 6. The minimum strain was taken as the benchmark; the strains at six points were normalized by this value. Points: (1) the midpoint of the iliopectineal line; (2) the central point of the acetabular inner plate; (3) the point on the sacral 1st vertebrae near the sacroiliac joint; (4) the point on the ilium of the sacroiliac joint as high as the sacral 1st vertebrae; (5) the iliac fossa; and (6) the highest point of the ischial notch.

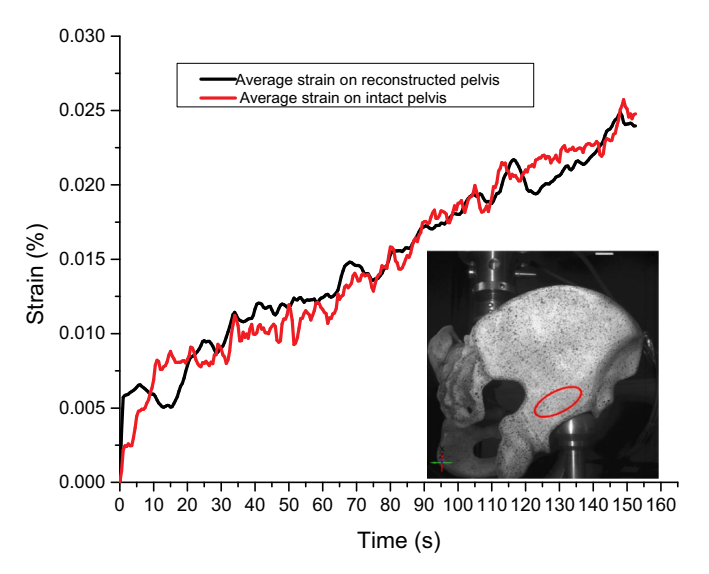


Fig. 7. The strain was 3 mm above the acetabulum.

3.3. Stabilization

The stability of the pelvis after reconstruction was assessed *via* the displacements of the left and right acetabulum. The vertical displacements are shown in Fig. 9. As the load increased, the displacement of both sides increased gradually, and the displacement on the contralateral side was slightly larger than that on the reconstructed side. The maximum displacement difference between the two sides was 0.209 mm. The average value (SD) of the difference between the two groups of data was 5.169e-2 (5.987e-2), and it was a clinically acceptable result.

The horizontal displacements were also investigated in this study. The axis perpendicular to the coronal plane was defined as the Z-direction. Considering the pubic symphysis plate loosens (Eastman et al., 2016), the prosthesis used in this study did not include the pubic symphysis plate. Thus, the displacements in the Z-direction of the left and right acetabula were different under the vertical load (Fig. 10). In the whole loading process, the maximum difference in the displacement in the Z-direction between the two acetabula was 0.324 mm. The displacement at 3 mm above the acetabulum was measured by the DIC

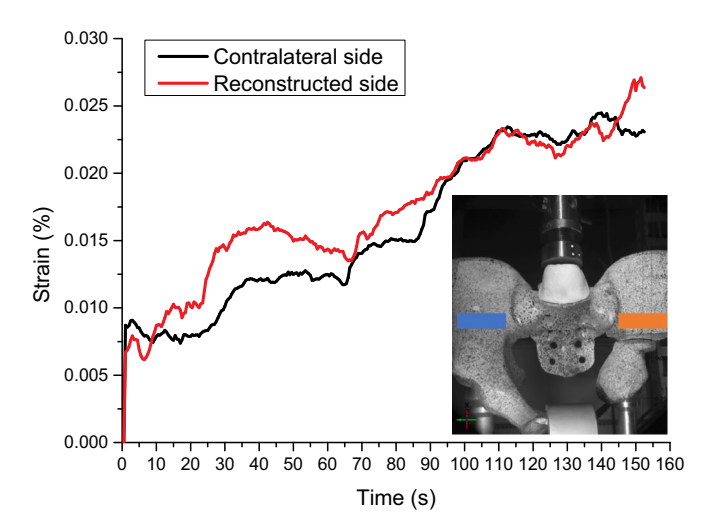


Fig. 8. The strain was 3 mm above the bone cutting plane on the reconstructed side and contralateral side.

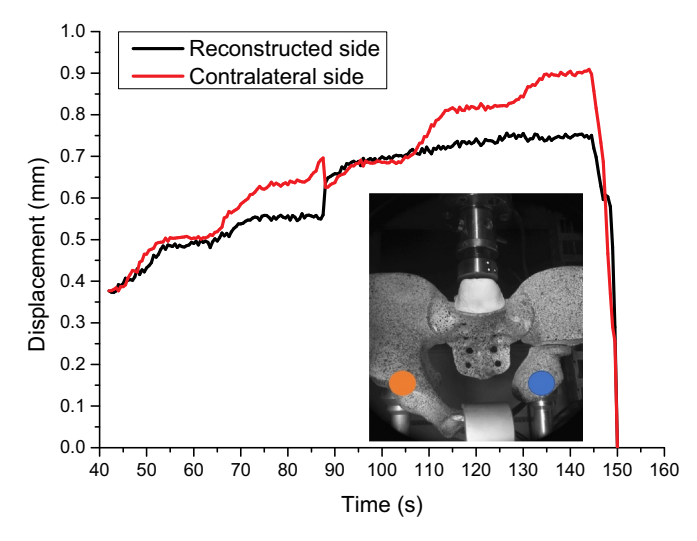


Fig. 9. The vertical displacements on the acetabulum after reconstruction.

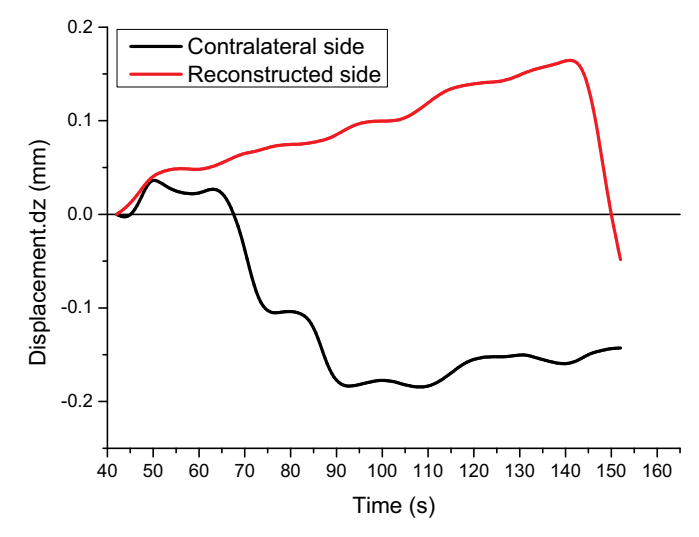


Fig. 10. The displacements in the Z-direction of the reconstructed and contralateral acetabula under the vertical load.

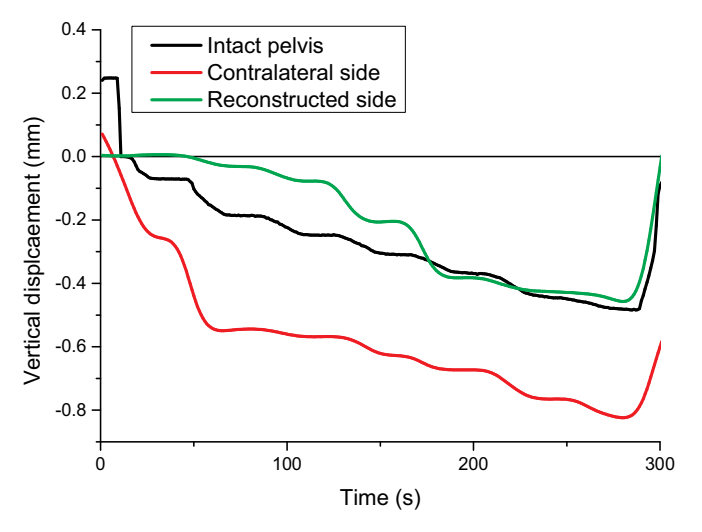


Fig. 11. The displacement was 3 mm above the acetabulum.

system; the result is shown in Fig. 11. The maximum difference on the contralateral side was 0.237 mm, and the maximum difference on the reconstructed side was 0.245 mm.

3.4. Failure load

In this study, the maximum load that the reconstructed pelvis can withstand was also measured. Using the mechanical testing machine, we continued to increase the vertical load until failure occurred. The failure load was 7.126~kN, which is 10~times the normal body weight (BW = 70~kg). A crack appeared at the superior of the intact acetabulum rather the reconstructed side (Fig. 12).



Fig. 12. The form of failure under ultimate load; the arrow indicates the location of the crack.

4. Discussion

The biomechanical properties of implant materials are important factors influencing the performance of implants (Dickinson et al., 2012). To accurately analyze the biomechanical properties of implants and reconstructive results in an artificial composite pelvic model, the mechanical conduction path in the artificial pelvis should be consistent with that of an in vivo pelvis. The mechanical conduction path in this artificial pelvic model traveled along the iliopectineal line and ischial notch. Moreover, the strains at the six points of measurement showed the same trend between the artificial pelvic model and the cadaveric pelvis. We found in our results that the composite pelvic model can effectively mimic the human pelvis, whereas in previous studies, the stiffness of the composite pelvis was significantly higher than that in cadaveric specimens (composite K = 1448 ± 54 N/m, cadaver $K = 832 \pm 62 \text{ N/m}$) (Girardi et al., 2016). Although the stiffness of the artificial pelvis is higher at some points, there are no significant differences in the strain trend at the selected points between the artificial and cadaveric pelvis. The results suggested that the use of an artificial pelvis in place of a cadaveric pelvis for mechanical experiments is effective and feasible.

In previous similar studies, a finite element simulation model was built by researchers to analyze the biomechanical performance of prostheses. However, finite element simulations have some unavoidable problems. Some simplified geometric features exist in finite element models that prevent the model from mimicking real mechanical properties. There is no standard method of selecting material parameters. The standard artificial bone models and DIC technique used in this study can be used to solve these problems. The displacement and strain of the whole field can be measured in experiments.

The complex spatial structure and important physiological functions of the pelvis present challenges for reconstruction. If the prosthesis used in this study can restore the mechanical properties of the pelvis, then patients with acetabular metastases who undergo reconstruction of the pelvic ring structure will have a good quality of life after surgery. Reconstruction of the acetabulum is a major surgical procedure, and it frequently results in multiple complications (Wunder et al., 2003). In previous studies on type II/II + III pelvic tumors, modular hemipelvic endoprostheses had satisfactory early clinical results (Guo et al., 2007). In our study, this prosthesis could be used to restore the physiological function of the pelvis. Comparing the strains before and after the osteotomy, it was found that the prosthesis had little effect on the contralateral side. By analyzing the strain at 3 mm on the horizontal plane of the osteotomy, we found that the strain level on the contralateral and reconstructed sides had high consistency under wide range of load. The reason for this result might be that the iliac bone supported by the modular hemipelvic endoprosthesis did not completely cover the bone cutting face. In this case, the force of the acetabulum prosthesis was not evenly distributed on the cross-section of the ilium. In addition, we kept increasing the load to meet the limit load of the pelvic model after the osteotomy. The failure load was 7.126 kN, and the crack was located in the superior of the acetabulum. In this failure load condition, the prosthesis system was intact without mechanical failure. This result suggest that the reconstruction of the SIJ fixed modular hemipelvic endoprosthesis is stable.

In this study, the pelvic prosthesis was not reconstructed on the pubic symphysis. In a previous study, researchers found that the pubic symphysis plate was prone to occur early postoperative breakage or loosening (Moed et al., 2012). The lack of a pubic symphysis plate might be the reason for the difference in the corresponding positions of the healthy and osteotomy sides. The displacement of the bilateral acetabulum indicated pelvic stability after the osteotomy. In the vertical direction, the displacement on both sides increased with the load. The small difference in the displacement between the two sides showed that the stability of this pelvic prosthesis was satisfying. Without the pubic symphysis plate, the displacements in the horizontal direction

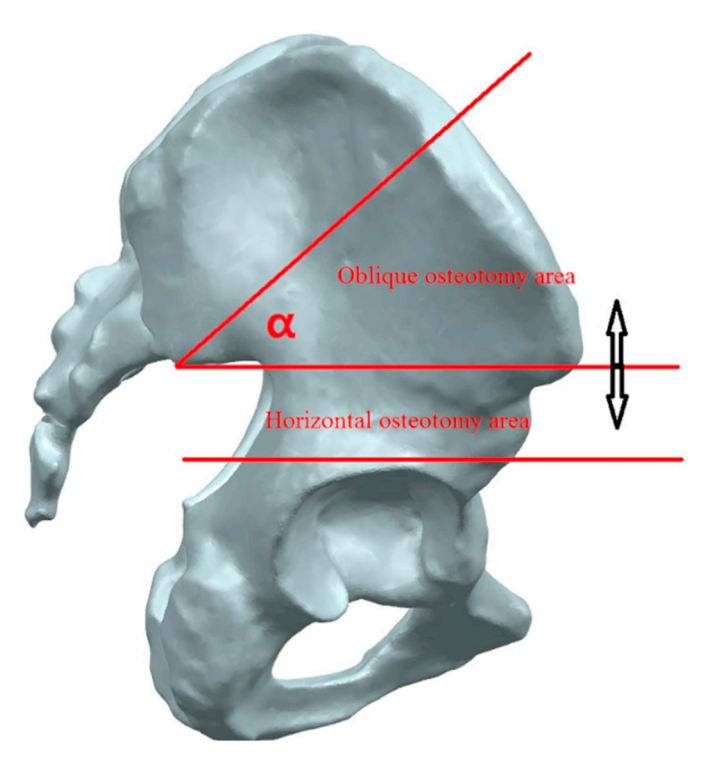


Fig. 13. The range of the osteotomy: from the distal rad line (horizontal) to the proximal rad line (oblique).

were in the opposite direction. However, the largest difference was acceptable, it had an insignificant influence on the stability of the pelvic structure. This result may be caused by the high stiffness of the artificial pelvic model. If the stiffness of the artificial pelvic model is more similar to that of the human body, it will more accurately reflect the prosthesis's physical performance.

Moreover, the mechanical experiment conducted in this study did not mimic the long-term use of implants. It is well known that osteointegration of the prosthesis is vital for longevity. The osseointegration surface of the prosthesis was made to be a 3D-printed porous structure to simulate bone trabeculae. Some studies have reported that the porous structure has a significant effect on bone ingrowth. Large pores ($500 \, \mu m$) are favorable for cell proliferation due to a better supply of oxygen and nutrients that enhance the survival and maintenance of biological activities. On the other hand, small pores ($200 \, \mu m$) are favorable for differentiation (Mygind et al., 2007). The size of the pores of the prosthesis used in this study was designed for bone ingrowth and manufactured by the *E*-beam technique, which has been proven to have sufficient accuracy to produce a porous structure with high quality bone ingrowth (Biemond et al., 2011).

The aim of reconstruction for type II/II + III resections has always been the restoration of a functionally stable hip joint. Although biological reconstruction, including iliofemoral arthrodesis, ischiofemoral arthrodesis, pseudarthrosis and a flail hip, has all been reported to yield good function, the occurrence of some drawbacks, such as prolonged immobilization, a leg length discrepancy and limited movement of the hip, warrant the development of improved surgical techniques. The reimplantation of devitalized autografts with THA also showed excellent functional outcomes but could not be used in patients with large tumors. Prosthetic reconstruction is therefore a reasonable treatment choice after type II/II + III resections (Liang et al., 2017).

It must be noted that due to the cost of this experiment, it was impossible to use multiple artificial pelvic bones for a large number of repeated tests. Although the prosthesis used in this study was manufactured with 3D-printing technology, it was a standard product with multiple sizes rather than a customized product. Therefore, the results

of pelvic reconstruction using the prosthesis that were shown in this study were similar to those in clinical practice. In this study, the artificial pelvic bone was made of an industrial product that has a similar mechanical property as a human pelvis, so the stability and repeatability of the results in this experiment were guaranteed. Based on the above conditions, we believe that the results of this experiment are important for reference of implant design and pelvic reconstruction clinically.

The osteotomy line is divided by the line through the posterior inferior iliac spine point and anterior superior iliac spine point. When the tumor area is below this line, the osteotomy line can be maintained horizontally, and a modular prosthesis of a size that matches the osteotomy height can be selected. When the tumor area progresses beyond the line, the surgeon can perform an oblique osteotomy and form a flat surface with an autologous bone graft from the femoral head (Fig. 13). The long screw that is attached the cup to the iliac fixation part can be passed through the autologous bone graft. This fixed method ensures the stability of the longitudinal structure.

It should be pointed out that the number of tests performed in this study was limited by the number of samples. According to clinical experience, in patients with a variety of bone tumors, the maximum angle of oblique osteotomy (α) is approximately 60 degrees. The effects of different α angles on the mechanical properties of the prosthesis were not studied in this paper. However, the mechanical structure around the prosthesis can be optimized by a horizontal osteotomy or oblique osteotomy with an autologous bone graft. Within the range of indications, the mechanical environment of the prosthesis is not significantly different. Moreover, the artificial pelvis used in this study was a standardized manufactured model that had mechanical properties that were consistent across the different samples. Therefore, the osteotomy type and loading conditions used in this study are representative, and the experimental results can be used to evaluate the performance of the prosthesis.

The experimental process showed that it is convenient to use non-contact, optical, 3D strain-measuring technology in mechanical experiments. To evaluate the performance of the SIJ fixed modular hemipelvic endoprosthesis in a pelvic structure, it is important to measure the strains and displacements at the points of interest. When used for this purpose, the DIC system is simple and easy to use.

In summary, the results of the mechanical study showed that this kind of prosthesis has good performance, but there is still room for improvement. In future implant designs, it is possible that the bearing area of the pelvic prosthesis on the osteotomy surface of the iliac bone can be expanded to achieve better loading patterns and reduce the negative effects of the unreconstructed pubic symphysis caused by a lower stability.

Acknowledgments

One author (JT) received funding from the National Key Research and Development Program of China (2016YFB1101502) and the Capital Health Research and Development of Special (No. 2018-2-4088), and the National Natural Science Foundation of China (No. 81872180).

References

Aboulafia, A.J., Buch, R., Mathews, J., Li, W., Malawer, M.M., 1995. Reconstruction using the saddle prosthesis following excision of primary and metastatic periacetabular tumors. Clin. Orthop. Relat. Res. 314 (314), 203–213.

Aljassir, F., Beadel, G. P., Turcotte, R. E., Griffin, A. M., Bell, R. S., & Wunder, J. S., et al. (2005). Outcome after pelvic sarcoma resection reconstructed with saddle prosthesis. Clinical Orthopaedics and Related Research, &NA;(438), 36-41.

Anderson, A.E., Peters, C.L., Tuttle, B.D., Weiss, J.A., 2005. Subject-specific finite element model of the pelvis: development, validation and sensitivity studies. J. Biomech. Eng. 127 (3), 364.

Bergmann, G., Deuretzabacher, G., Heller, M., Graichen, F., Rohlmann, A., Strauss, J., Duda, G.N., 2001. Hip contact forces and gait patterns from routine activities. J.

X. Li. et al.

- Biomech. 34, 859-871.
- Biemond, J.E., Hannink, G., Verdonschot, N., et al., 2011. The effect of E-beam engineered surface structures on attachment, proliferation and differentiation of human mesenchymal stem cells[J]. Biomed. Mater. Eng. 21 (5–6), 271.
- Cottias, P., Jeanrot, C., Vinh, T.S., Tomeno, B., Anract, P., 2001. Complications and functional evaluation of 17 saddle prostheses for resection of periacetabular tumors. J. Surg. Oncol. 78 (2), 90–100.
- Dalstra, M., Huiskes, R., 1995. Load transfer across the pelvic bone ★. J. Biomech. 28 (6), 715–724
- Dickinson, A. S., Taylor, A. C., & Browne, M., (2012). The influence of acetabular cup material on pelvis cortex surface strains, measured using digital image correlation. J. Biomech., 45(4), 0–723.
- Eastman, J.G., Krieg, J.C., Routt, M.L.C., 2016. Early failure of symphysis pubis plating. Injury S0020138316301917.
- Enneking, W.F., Dunham, W.K., 1978. Resection and reconstruction for primary neoplasms involving innominate bone. J. Bone Joint Surg. 60 (6), 731–746.
- Falkinstein, Y., Ahlmann, E.R., Menendez, L.R., 2008. Reconstruction of type ii pelvic resection with a new peri-acetabular reconstruction endoprosthesis. Journal of Bone and Joint Surgery - British Volume 90–B (3), 371–376.
- Girardi, B.L., Attia, T., Backstein, D., Safir, O., Willett, T.L., Kuzyk, P.R.T., 2016. Biomechanical comparison of the human cadaveric pelvis with a fourth generation composite model. J. Biomech. 49 (4), 537–542.
- Guo, W., Li, D., Tang, X., Yang, Y., Ji, T., 2007. Reconstruction with modular hemipelvic prostheses for periacetabular tumor. Clin. Orthop. Relat. Res. 461 (461), 180–188.
- Hao, Zhixiu, 2011. The effect of boundary condition on the biomechanics of a human pelvic joint under an axial compressive load: a three-dimensional finite element model. J. Biomech. Eng. 133 (10), 101006.
- Harrington, K.D., 1981. The management of acetabular insufficiency secondary to metastatic malignant disease. J. Bone Joint Surg. Am. 63–A, 653–664.
- Hillmann, A., Hoffmann, C., Gosheger, G., R?Dl, R., Winkelmann, W., & Ozaki, T., 2003. Tumors of the pelvis: complications after reconstruction. Arch. Orthop. Trauma Surg.

- 123 (7), 340-344.
- Ji, T., Guo, W., Yang, R.L., et al., 2013. Modular hemipelvic endoprosthesis reconstruction-experience in 100 patients with mid-term follow-up results[J]. European Journal of Surgical Oncology (EJSO) 39 (1), 53-60.
- Liang, H., Ji, T., Zhang, Y., et al., 2017. Reconstruction with 3D-printed pelvic endoprostheses after resection of a pelvic tumour[J]. Bone & Joint Journal 99–B (2), 267–275
- Moed, B.R., Grimshaw, C.S., Segina, D.N., 2012. Failure of locked design-specific plate fixation of the pubic symphysis: a report of six cases. J. Orthop. Trauma 26 (7), e71.
- Mygind, T., Stiehler, M., Baatrup, A., Li, H., Zou, X., Flyvbjerg, A., Kassem, M., Bunger, C., 2007. Mesenchymal stem cell ingrowth and differentiation on coralline hydroxyapatite scaffolds. Biomaterials 28, 1036–1047.
- Natarajan, M.V., Bose, J.C., Mazhavan, V., Rajagopal, T.S., Selvam, K., 2001. The saddle prosthesis in periacetabular tumours. Int. Orthop. 25 (2), 107–109.
- Uchida, A., Myoui, A., Araki, N., Yoshikawa, H., Ueda, T., Aoki, Y., 1996. Prosthetic reconstruction for periacetabular malignant tumors. Clin. Orthop. Relat. Res. 326, 238–245.
- Windhager, R., Karner JKutschera, H.P., Polterauer, P., Salzer, K.M., Kotz, R., 1996. Limb salvage in periacetabular sarcomas: review of 21 consecutive cases. Clinical Orthopaedics & Related Research 331 (331), 265–276.
- Wunder, J.S., Ferguson, P.C., Griffin, A.M., Pressman, A., Bell, R.S., 2003. Acetabular metastases: planning for reconstruction and review of results. Clin. Orthop. Relat. Res. 415. S187–S197.
- Xiu, P., Jia, Z., Lv, J., Yin, C., Cheng, Y., & Zhang, K., et al. (2016). Tailored surface treatment of 3d printed porous ti6al4v by micro-arc oxidation for enhanced osseointegration via optimized bone in-growth patterns and interlocked bone/implant interface. ACS Applied Materials & Interfaces, acsami.6b05893.
- Xu, D., Wang, Y., Jiang, C., Fu, M., Li, S., & Qian, L., et al. (2018). Strain distribution in the anterior inferior tibiofibular ligament, posterior inferior tibiofibular ligament, and interosseous membrane using digital image correlation. Foot & Ankle International, 107110071775316.